Available online at www.sciencedirect.com
SCIENCE DIRECT®
Journal of Nuclear Materials 349 (2006) 57–82
journal of nuclear materials
www.elsevier.com/locate/jnucmat

Thermodynamics of the O–U system: III – Critical assessment of phase diagram data in the U–UO_{2+x} composition range

Mehdi Baichi [a,1], Christian Chatillon [b,*], Gérard Ducros [a], Karine Froment [c]

[a] CEA Cadarache/DEN/DEC/S3C/LARA, Centre de Cadarache, 13108 Saint Paul Lez Durance, France
[b] Laboratoire de Thermodynamique et Physico-Chimie Métallurgiques, (UMR 5614, CNRS/UJF/INPG) E.N.S.E.E.G., BP. 75 38402 Saint Martin d'Hères, France
[c] CEA Grenoble/DTN/SE2T/LPTM, 17 rue des Martyrs, 38054 Grenoble cedex 9, France

Received 14 April 2005; accepted 5 October 2005

Abstract

In order to help understand the behavior of the UO_2 fuel in a severe nuclear accident, the phase diagram data of the O–U system in the U–UO_2 composition range are reviewed critically, so that the most reliable set of original data can be selected. In the course of this assessment, a special effort is made to evaluate as realistically as possible the associated uncertainties, not only for reliable data selection, but also as weights in the procedure, which is used later to optimize phase diagram and thermodynamic data. Among the criteria for selection, the non-congruent vaporization of the $UO_{2\pm x}$ phase and the interactions between UO_2 and the containment materials are discussed, together with a detailed analysis of the experimental techniques used. A melting temperature for UO_2 of 3138 ± 15 K is proposed, which is compatible with the selected data for the liquidus and solidus temperatures in this composition range. The solubility limit of oxygen in liquid uranium is selected as the smallest value among different and largely non-consistent values, and this selection leads to the existence of a large miscibility gap in the liquid phase between one metal rich liquid and one oxide rich liquid.

1. Introduction

In a severe accident within a nuclear power plant, the high temperature behavior of the fuel as well as its interactions with the cladding materials are important chemical features that govern the formation of different vapor, liquid and solid phases, that in turn could lead to phase separation and consequently to the so-called 'delocalisation' process, i.e. a mechanical collapse of parts of the reactor core. In this process, the thermodynamic description of basic binary and ternary or more complex chemical systems based on uranium is an important tool in the predicting of phases that can be formed not only in quasi-equilibrium conditions after a given

* Corresponding author.
E-mail addresses: mehdi@baichi.net (M. Baichi), chatillon@ltpcm.inpg.fr (C. Chatillon).
[1] Present address: IRSN, BP. 17, 92260 Fontenay-aux-Roses cedex, France.

0022-3115/$ - see front matter © 2005 Elsevier B.V. All rights reserved.
doi:10.1016/j.jnucmat.2005.10.001

time but also in terms of local equilibria enabling the identification of the chemical forces that drive different kinetic phenomena such as diffusion, convection or interfacial reactions including vaporization.

This paper is the first of this series dedicated to the very high temperature thermodynamic behavior of the UO_2 fuel. Its aim is to collect and critically assess the published phase diagram data in the U–UO_2 range of the U–O system, which includes an additional thermodynamic and phase diagram optimization using the Parrot software [1]. In this least square fit procedure, weightings are given for each original data point which are, in principle, based on the uncertainties attributed to these data. For this reason, efforts have been made not only to analyze and select the most reliable data, but also in the estimate of their associated uncertainties. This paper forms part of the doctorate studies of one of the authors (Baichi) [2], and will be followed by the assessment of the published thermodynamic data. The above mentioned doctorate studies are complementary to those of Labroche [3] on the UO_2–U_3O_8 range of the U–O system.

2. Criteria for data and uncertainty analysis

2.1. Rules for the treatment of uncertainties

In the U–UO_2 system, the two main quantities that are measured for the determination of the phase diagram are:

(1) the composition, often analyzed as $UO_{2\pm x}$ or $O/U = x$ with the associated uncertainty δx and
(2) the temperature (T), always measured by pyrometry due to the very high temperatures of melting.

2.1.1. Compositions

Composition analysis of the samples may be performed by gravimetry either after reduction with pure H_2 at $T > 1173$ K [4] to $UO_{2\pm0.001}$ or by oxidation to U_3O_8(s) at atmospheric pressure. For this last case, Labroche et al. [3,5] proposed an analysis of the different causes of errors, based on the Ackermann and Chang [6] work on the non-stoichiometry of the compound U_3O_{8-z}. The main goal of this analysis was to determine compositions obtained:

(1) by oxidation in air or in pure O_2 or $Ar + O_2$, that is by gravimetry after cooling and
(2) by oxidation in situ with a thermobalance at constant temperature (thermogravimetry).

For oxidation at constant temperature in a thermobalance, a formula was proposed and used in this paper for correction of non-stoichiometry of the final oxide U_3O_{8-z}, when oxidation is performed at $T > 873$ K. For gravimetry after cooling, we have chosen to split the correction into two parts:

(i) 50% is used to correct the authors' composition values and
(ii) the other 50% is added to the causes of uncertainty. The reason for this choice is that there is very often no real information about the cooling speed to warrant the complete stoichiometry recovering as observed by thermogravimetry when cycling the temperature [7,8]. The different uncertainties for composition analysis are summarized in Table 1.

In the course of the experiments performed for phase diagram analysis, different causes for uncertainties have to be taken into account, for example

- The influence of humidity on the UO_2 sample, especially when used as a powder. To avoid this, several authors used sintered pellets that are less reactive. According to Schaefer [4], the influence of humidity, when controlled, gave $\delta x = \pm 0.002$.
- For the reaction of precipitated U metal with air for UO_{2-x} hypostoichiometric samples after cooling: $\delta x = \pm 0.002$ is taken.
- The reaction of predominately hyperstoichiometric UO_{2+x} with the containers at high temperature [9]. For the chemical analysis of the samples after cooling, it was necessary to subtract a contribution from the impurities (such as W, Re) and their oxides in the resulting O/U composition ratio. According to Latta and Fryxell [9] $\delta x = \pm 0.01$.

To take into account the different causes of uncertainty – carefully chosen as independent –, we use the law of propagation of errors as in Ref. [10]. For example in case of composition $O/U = x$, the relation given below can be written,

Table 1
Intrinsic uncertainties as summarized from Refs. [3–5] attributed to different analytical techniques used to measure the O/U (=x) composition ratio

Analytical technique	Uncertainty $\delta x = \delta(O/U)$
Polarography	±0.005
Coulometry	±0.003
Gravimetry and thermogravimetry without correction for non-stoichiometry as done in this work	±0.003
Fusion in inert gas	±0.006
Reduction by H_2 at $T > 1173$ K	±0.001

$$\delta x_{\text{total}} = (\delta x^2_{\text{exp}} + \delta x^2_{\text{ref}} + \delta x^2_{\text{humidity}} + \delta x^2_{\text{air}} + \delta x^2_{\text{container}})^{1/2} \quad (1)$$

exp is from the original data as published and is often quoted as the reproducibility, ref is for the composition of the final product, i.e. for oxidation U_3O_8 or for reduction under H_2 atmosphere UO_2, and humidity and air may be alternatively used. According to uncertainties in Table 1, a minimum total value $\delta x = \pm 0.015$ is obtained without the contribution of the reference compound. Further, the total uncertainty will be estimated according to each experimental method.

2.1.2. Temperature

The pyrometric measurements were performed either on open systems for which the vapors may change the emissivity, or on closed systems with a cavity machined in the walls and used as a black body. This later way is retained as the most reliable method to measure the temperature. Some pyrometers were calibrated at NBS (presently NIST) with δT from 15 to 30 K or checked by measuring melting points of secondary standard materials in the same device as for UO_2 measurements. In the case of secondary melting points, δT_{ref} was firstly calculated as a mean value of the observed deviations in the calibration runs. Finally, we add to this δT_{ref}, using the law of propagation of error, the original uncertainties of the authors or an estimate based on similar measurements.

2.2. Chemical criteria in the data analysis

2.2.1. Congruent vaporization

The first chemical criterion is related to the behavior of the UO_{2-x} or $U + UO_{2-x}$ samples when analyzed in open systems. Many authors observed that the samples showed composition changes due to vaporization processes [11,12], even in Ar or He atmospheres, or even when total time for analysis was shortened to 20 s [13]. These composition changes are related to mass losses due to vaporization, the vapor composition being different from that in the condensed phase. These features are clearly demonstrated in mass spectrometric determinations of partial pressures [14,15]; for 2250 K (Fig. 1): the total pressure or similarly the total effusion flow under vacuum conditions shows a minimum for a UO_{2-x} composition different from that of stoichiometric UO_2.

This minimum corresponds to an azeotropic or congruent vaporization [16,17] composition. Any sample the composition of which is richer with oxygen than the congruent one will move by matter loss [18,19] toward the congruent composition. For the same reason, a sample richer in U than the congruent composition will loss an excess of U (via UO(g)

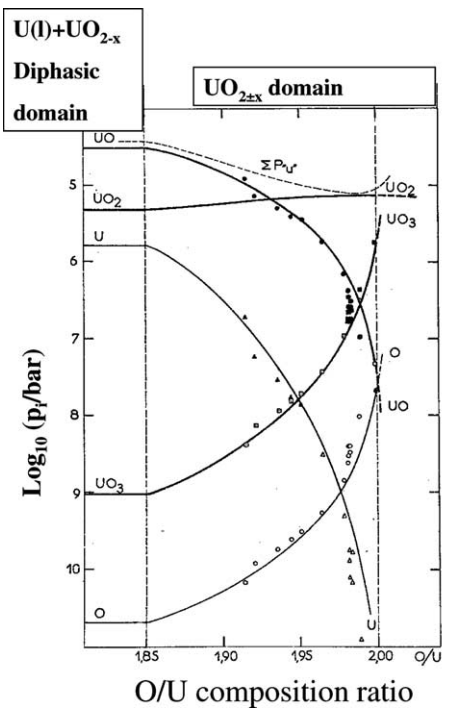

Fig. 1. Isothermal experiment performed by Knudsen cell mass spectrometry [14,15]. The partial vapor pressures vary considerably in the non-stoichiometric UO_{2-x} domain, and the total pressure has a minimum for UO_{2-x} which corresponds to an azeotropic composition. For this composition the gas and the solid phases have the same composition. Full symbols are for measured partial pressures; empty symbols are for calculated partial pressures from known equilibrium constants as measured by the authors.

mainly), and finally will reach the congruent composition. These properties have been used:

- by Pattoret et al. [14,15] and Pattoret [20] in mass spectrometric determinations, using calibration procedures based on composition scaling between the analyzed initial composition before experiment and the final congruent composition,
- by Edwards et al. [21] in effusion measurements with analysis of the O/U ratio of the residues in order to propose a congruent composition line in the UO_2 non-stoichiometric domain (Fig. 2).

Working with open systems and with V shaped tungsten ribbon heated by the Joule effect, small samples in Ar, He or Ar + H_2 atmospheres, Bannister [22] observed changes in composition that was attributed to composition differences between vapor and condensed phases, in agreement with this analysis, meanwhile Bates [23] attributed these changes to impurities in Ar ($p(O_2) = 10^{-6}$ bar, or $p(H_2O) = 10^{-5}$ bar) acting either during temperature cycling or during intermediate temperature plateaux.

The pressures of the impurities are compared with the UO_2(g) pressure (the most important species at the congruent composition, other species being lower by a factor of about 10) calculated in compilation of Younés [24] or from the data of Ackermann et al. [25] (the two relations lead to similar values) and given in Table 2. One can see that the pressures of the above mentioned gaseous impurities are generally at least 100 times lower than any vaporization partial pressures at the melting temperatures, therefore they could not shift the melting composition by their dissolution. For the highest temperatures of the intermediate heat treatments between two melting observations the difference is not always so large, and we can postulate that the sample can be enriched in oxygen. Thus, even if

Table 2
UO_2(g) partial pressures over the congruent vaporization composition of OU_{2-x} as calculated from Younés data [24] for comparison purpose with $p(O_2)$ and $p(H_2O)$ impurities (10^{-6} and 10^{-5} bar respectively)

Heat treatment Bates [23] T (K)	Calculated pressure Younés [24] $p(UO_2)$ (bar)	Melting temperature Bates [23] T (K)	Calculated pressure Younés [24] $p(UO_2)$ (bar)
1873	9.62E−09	3023	1.84E−02
–	–	3025	1.87E−02
–	–	3002	1.56E−02
2073	3.77E−07	3118	3.77E−02
–	–	2960	1.11E−02
2273	7.74E−06	3008	1.63E−02
2473	9.75E−5	2976	1.27E−02
2543	2.15E−04	2945	9.85E−03
2673	8.41E−04	2948	1.01E−02

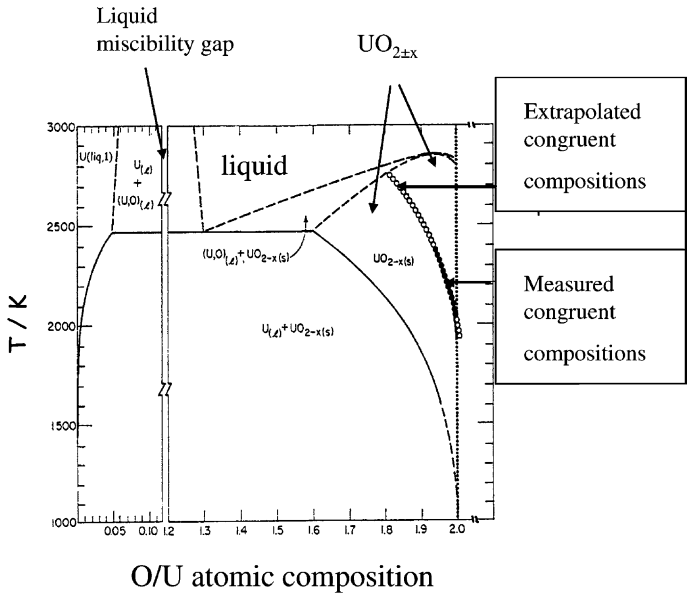

Fig. 2. Congruent vaporization line in the UO_{2-x} domain as obtained from Knudsen effusion [21]. (●) experimental data, (○) extrapolated data according to the proposed formula by the authors.

the lower temperature treatments between two measurements of solidus or liquidus temperatures can catch gas impurities, the UO_{2-x} samples which return to the high temperature range of the thermal analysis could change their composition more quickly and 'freely' by vaporization towards the congruent one along the solidus line.

The changes in composition of samples in experiments toward congruent vaporising compositions (CVC) can be analyzed in order to give specific CVC's compositions, which can be used in thermodynamic treatments as independent data. From Bates [23] data, the two trajectories 1 and 2 for temperature cycling (Fig. 3) of original samples with $O/U = 1.97$ and 1.927, led to the same final composition, $O/U = 1.94 \pm 0.02$ (according to Bates), located in principle on the solidus line. This composition corresponds to the intercept of the UO_{2-x} azeotropic (or congruent) line with the solidus. We observe also that this O/U ratio is clearly different from the one proposed by Edwards et al. [21] by extrapolation: the difference is probably due partly to the Knudsen flow relation used that is no longer valid in the Bates experiments because the total pressure exceeds clearly the molecular flow regime in the reactor. The exact nature of this difference will be analyzed in a further study from results of the optimization of phase diagram and thermodynamic data. Indeed, Edwards et al. [21] were not successful in the use of congruent relations to solve vapor phase thermodynamic discrepancies, because a full thermodynamic description of the $UO_{2\pm x}$ non-stoichiometric domain must be obtained as a first and independent step before analysis of vapor phase behaviour.

In the liquid phase, for a temperature close to or along the liquidus line, Bates [23] observed that the congruent composition is between $O/U = 1.78$ and 1.927, which is in reasonable agreement with the data of Anderson et al. [26]; $O/U = 1.86 \pm 0.02$ and of Rothwell [27]; $O/U = 1.885 \pm 0.01$. These latter values were obtained when maintaining a liquid UO_2 sample under Ar for a long time at a temperature slightly above the melting one point in an electric discharge furnace, and are shown in Fig. 3. Uncertainties either come from the authors or are evaluated according to relation 1, using a correction for calcination temperature. It is important also to quote that in such experiments, performed as a totally open system, any impurities in the neutral atmosphere can enrich the liquid phase with oxygen, and consequently these experimental values can be higher O/U values for the azeotropic compositions of the liquid.

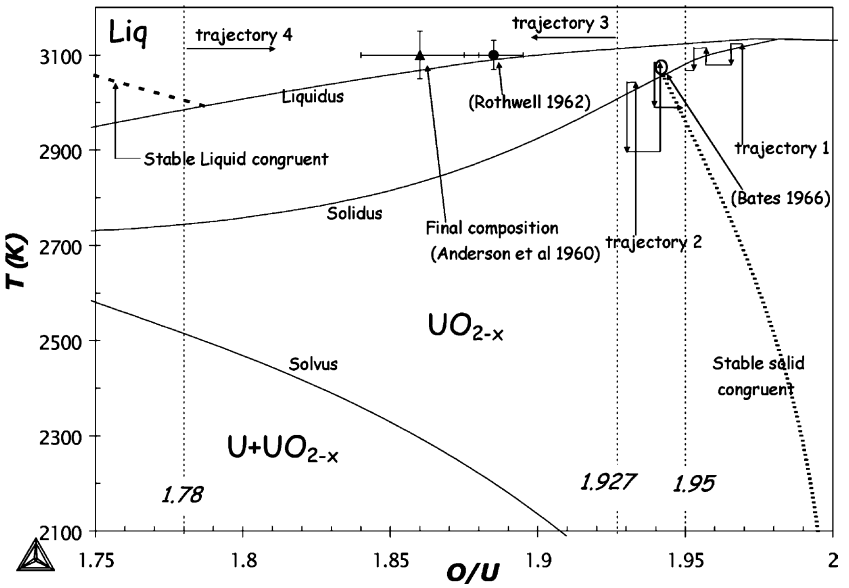

Fig. 3. Schematic representation of the composition changes due to vaporization losses as observed by Bates [23] during temperature cycles close to the determinations of solidus temperature when starting from O rich compositions (trajectory 1) or from U rich compositions (trajectory 2). The final composition is always 1.94 ± 0.02. For the liquid, trajectories 3 and 4 were explored: Anderson et al. [26] obtained a final composition 1.86 ± 0.02 by heat treatment of the liquid phase, and similarly Rothwell [27] obtained 1.885 ± 0.01. Stable solid and liquid congruent lines were calculated from thermodynamic data in Ref. [28].

The relative position of the solid and liquid congruent lines has been already calculated for the As–Ga system [29] in which the transition from the congruent compound AsGa to the liquid was also observed in the measurements of thermodynamic properties or the determination of the phase diagram. Thermodynamic arguments can be developed to analyze the relative positions of the congruent lines when crossing the two phase domain liquid ↔ solid solutions in the following way. In Fig. 4, at the intercept S of the solid congruent line with the solidus, the vapor composition equals the solid UO_{2-x} composition at S. Meanwhile the first liquid droplet formed according to the tie line has a composition L_1 richer in U than the solid with which it is in equilibrium. Increasing slightly the temperature or causing the solid phase to disappear, the liquid at L_1 will vaporize with a vapor composition richer in oxygen (vapor composition must be the same as in point S, due to the equality of chemical potentials all along the line). Consequently any liquid sample with a composition close to L_1 will move by vaporization losses towards compositions as L_2 richer in U. At this point, the vapor composition becomes richer in U, and the liquid phase will reach its own congruent line by loss of the excess of oxygen. Thus, we can deduce that the liquid congruent line is necessarily in the U rich side of the L_1–S tie-line, and the UO_2 stoichiometric compound cannot vaporize congruently, not only in the solid phase as observed experimentally but also, and with a $O/U << 2$ composition, in the liquid phase. According to this thermodynamic analysis, the congruent composition as determined by Anderson and al. [26] in the liquid phase should be compatible with the tie-line L_1–S based on the S composition as determined by Bates [23]. This constraint must be compatible with our present selection of phase diagram data.

The present analysis shows that we cannot retain phase diagram data performed under these conditions because uncontrolled composition trends are occurring. By considering these uncontrolled changes of composition, the selected data must only be taken from investigations using closed systems.

2.2.2. Chemical compatibility of UO_2 with containers

Owing to the very high temperature range of any phase diagram or thermodynamic data determination in the U–UO_2 system, difficulties were encoun-

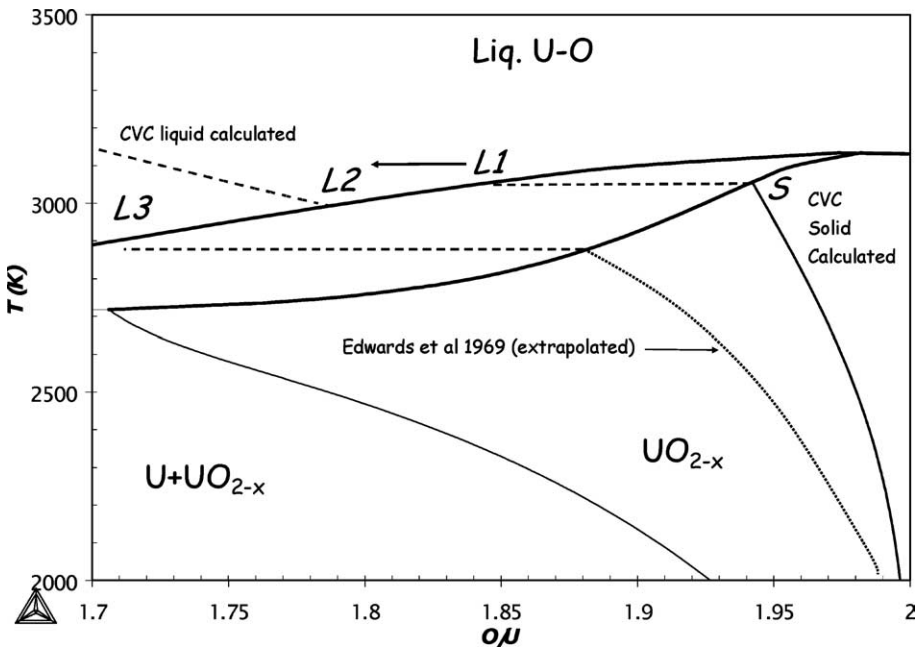

Fig. 4. Relative positions of the solid and liquid congruent compositions for vaporization (CVC as explained in the text) as a function of solid–liquid equilibria represented by tie-lines. We observe some discrepancies between the extrapolated Edwards et al. [21] solid congruent line and the Bates [23] and its agreement with the liquid azeotropic compositions of Anderson et al. [26] and Rothwell [27] data, which have already been presented in Fig. 3.

tered with the U–UO_2/container interactions from the beginning of the high temperature studies because U is very reactive and difficult to contain. Tungsten appears to be the best material container, at least in the U–UO_2 range, but still the physico-chemical compatibility remains dependent on the quality of the sintered tungsten and sometimes of the machining process (electro-erosion machining may result in the presence of carbon residues). For the study of the $UO_{2\pm x}$ solidus–liquidus domain, Latta and Fryxell [9,30] used W or Re, and showed that a non-negligible dissolution of these materials exists in the liquid UO_{2+x} using post microscopic observations of some U_xWO_3 inclusions that were characterised by independent chemical analysis of precipitated W impurities. With Re, some dissolution in the liquid UO_{2+x} was also observed and it seems that there is no other more satisfactorily materials available for the containment of these materials of the U–O system. The O/U ratio analysis performed by Latta and Frixell before and after experiments – taking off the precipitation of tungsten complex oxides – show a posteriori that oxygen leaks are probably weak in their tungsten and rhenium containers.

Tantalum has been used [15,31] but some continuous dissolution of U and O is assumed from different experimental observations. In vapor pressure measurements with Knudsen cells, the vapor phase compositions as observed by mass spectrometry are clearly different over $UO_{2\pm x}$ in Ta or W cells, showing a more reducing vapor composition with Ta containers, a consequence of oxygen leak through the walls [15]. Edwards et al. [21] finally tested the behavior of an initial UO_2 stoichiometric sample maintained a long time at high temperature in a welded W vessel. Composition analysis after the experiment run at 2427 K showed that $UO_{2.000\pm0.004}$ composition did not change appreciably, and dissolved W in urania is <0.005 wt%. This result shows that oxygen does not leak or diffuse in these conditions through tungsten. Younés [24] in his thesis underlined that the use of tungsten may depend on the quality of the material, and in case of good quality tungsten, the lack of independent successful oxygen diffusion coefficient determinations in literature a well as reliable solubility values proves a contrario that oxygen do not diffuse appreciably in. Moreover, any increase of the oxygen potential will precipitate the WO_{2-x} oxide phase or a complex oxide as observed by Latta and Frixell. Conversely, for Ta the oxygen leak (by diffusion) is probably associated with a known large solubility of oxygen in tantalum at high temperature.

As a conclusion, experiments run with W can be regarded as the most reliable, but must be also checked by final analysis of the O content as well as of W (or Re) dissolved in $UO_{2\pm x}$ sample as carried out by Latta and Fryxell [9,30]. Such analyses allow the determination of the $UO_{2\pm x}$ composition after calcination with corrections for the presence of these impurities. Experiments run with Ta must be carefully analyzed when performed at high temperature before retaining any data.

3. Liquidus and solidus in the $UO_{2\pm x}$ range

The difficulties in the measurements of the melting temperature of UO_2 due to the complex chemistry of the compound, problems with containment materials and the very high temperature range involved are illustrated by the history of the results shown in Fig. 5 and Table 3.

Finally, the IAEA assessors proposed $T_{\text{melting}} = 3116 \pm 25$ K from Ref. [47], but without any justification in this reference. With the criteria used in this study, – i.e. closed systems, W containers and black body pyrometric conditions must be used – the results of only five authors from Table 4 have been used to obtain a mean value for the melting temperature of UO_2, $T_{\text{melting}} = 3134 \pm 22$ K. However, this value will be revised later in this paper after selection of liquidus and solidus data to be consistent with the phase diagram and thermodynamic data selection for the final optimization procedure.

The liquidus and solidus were measured by three authors [9,22,23,30] as illustrated in Fig. 6(a), and their method of measurement is summarized in Table 3. Large discrepancies occur between results obtained with open systems such as V shaped tungsten filaments [22,23] and with closed vessels [9,30] so that the different resulting liquidus and solidus data are not separable. Following the preceding analysis given in part 2 of this paper, only the data from investigations in closed tungsten vessels of Latta and Fryxell [9,30] are retained. However, the dissolution of W and Re in the $UO_{2\pm x}$ liquid leads to a decrease in the melting temperature, and for this reason the original liquidus data are corrected according to the Raoult's cryoscopic law, with the relation

$$\Delta T = \frac{RT^2(\text{melting}, UO_2)}{\Delta H_{\text{melting}}(UO_2)} \tag{2}$$

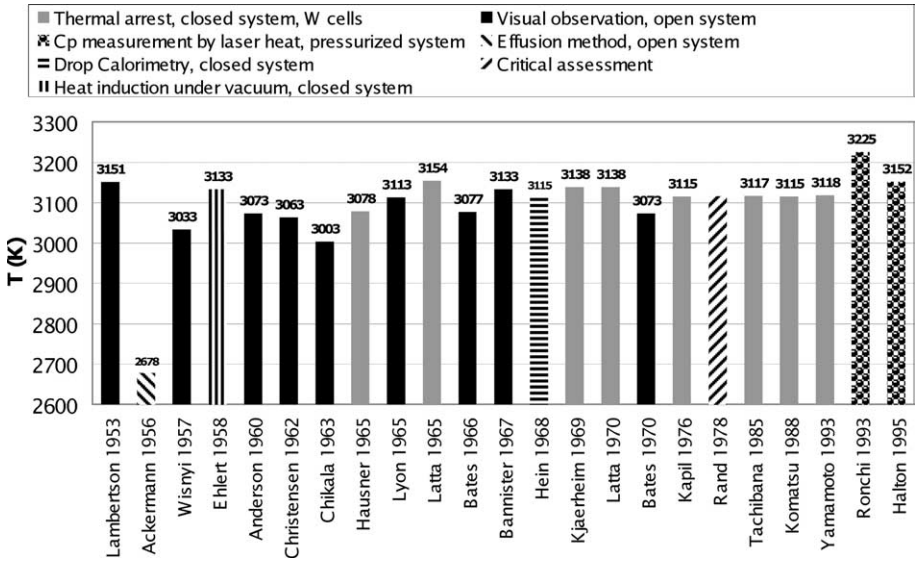

Fig. 5. Historical evolution of experimental data for the melting temperature of UO_2. The very large discrepancies observed are derived partly from difficulties in temperature measurements and partly from the chemical behavior of $UO_{2\pm x}$ compound, vaporization and reactivity with the containments or the atmospheres.

in which R is the ideal gas constant, T and ΔH the melting temperature and enthalpy as determined from Hein et al. [49,50] and Leibowitz et al. [51,52] (3138 K, 75.4 kJ mol^{-1}). The molar fraction x of W or Re in the liquid $UO_{2\pm x}$ is given by Latta and Fryxell [9,30], after post experiment chemical analysis and the solubility of W and Re (or their oxides) in the solid phase is assumed negligible. The corrected liquidus results are presented in Table 5. Some corrections as high as 87 K, corresponding to high oxygen content, are observed.

Owing to the complexity of the composition analysis after the experiments, and especially the first step corresponding to W and Re analysis, the authors propose an uncertainty for the O/U ratio of $\delta x = \pm 0.01$. However, the calcination at 1173 K into U_3O_8(s) is not described and a supplementary contribution of $\delta x_{\text{corr}} = \pm 0.02$ is attributed to the uncertainty based on the work of Ackermann and Chang, as already explained by Labroche et al [5]. Finally, the total composition uncertainty is calculated from

$$\delta x_{\text{Latta and Fryxell}} = \sqrt{(\delta x^2_{\text{author}} + \delta x^2_{\text{corr}})} = \pm 0.022. \quad (3)$$

The temperature uncertainty proposed by the authors, $\delta T = \pm 15$ K is retained because of their calibration procedure and experimental method employed. The final retained data for the liquidus together with their associated uncertainties are presented in Fig. 6(b). In order to impose consistency between these liquidus and solidus data and the melting temperature of UO_2, the melting temperature of Latta and Fryxell is ultimately preferred: T(melting, UO_2) = 3138 ± 15 K. It will be noted, from Table 4, that this value is fully consistent with the most probable experimental one. For the monotectic temperature, the value proposed here is that of Latta and Fryxwell [9]: 2701 ± 15 K; this value is in agreement with the value of Bannister [22].

Recently, Manara et al. [48,49] used a high pressure cell – up to 0.25 Gpa of an inert or doped oxygen gas mixture – in which they observed the melting behaviour of a part of the surface of a UO_{2+x} sample under two series of Laser shots. After stopping part of the Laser shots, pyrometric thermal analysis (by temperature decrease) of a stoichiometric UO_2 sample reveals a clear thermal arrest. For UO_{2+x} samples a first break is attributed to the liquidus temperature, and a second break at lower temperature attributed to the solidus. First the evolution of the melting temperature of stoichiometric UO_2 as a function of the applied total pressure (for values >0.05 GPa) is analysed that gives

Table 3
Melting temperature as measured for UO_2 from literature with experimental conditions

Authors year [Refs.]	Melting temperature (K)	Experimental technique	Sample preparation and container	Sample analysis
Lambertson and Mueller (1953) [32]	3151 ± 22	• Visual observation of the first droplet • Vacuum or He (1 bar) furnace in W • Quenching in liquid N_2	• UO_2(99.9%), sintered at 1873–2023 K, H_2 • W crucibles (open)	• XRD • MEB • Chemical analysis
Ackermann et al. (1956) [11]		• Mass spectrometry with Knudsen cell	• O/U << 2	
Wisnyi and Pijanowski (1957) [33]	3033 ± 30	• Visual observation of the first droplet • W ribbon furnace (V shaped) • He, Ar or H_2 (1 bar)	• Open system in W	• XRD before and after
Ehlert and Margrave (1958) [34]	3133 ± 45	• Emissivity measurement • Vacuum • Graphite induction furnace	• O/U = 2 (initial) • Open system in carbon	
Anderson et al. (1960) [26]	3073 ± 100	• Visual observation of the first droplet • Arc melting (W and Fe electrodes)	• O/U = 2 • Open system in W/Fe	• XRD post analysis
Christensen (1962) [13]	3063 ± 20	• Visual observation by microscope of the first droplet • V shaped W ribbon furnace • He (1 bar)	• UO_2 95% density • Sintered at 2033K, H_2 (1 bar) • Open system in W	• Analysis of the irradiation effects (burning rate)
Chikalla (1963) [35]	3003 ± 30	• Emissivity measurements and droplet observation • V shaped W ribbon furnace • He (1 bar)	• UO_2 sintered in H_2 at 2000 ppm H_2O • Open system	• XRD
Hausner (1965) [36]	3078 ± 15	• Thermal arrest by decreasing temperature • Induction furnace tested for thermal gradient	• UO_2 natural or enriched • W closed container	
Lyons et al. (1965) [37]	3313 ± 20	• Joule heating and thermal arrest by decreasing temperature • Ar (13.5 bar)	• UO_2 or UO_{2-x} (8g) • W closed container (0.5–0.7 mn wall thickness)	
Latta and Fryxell (1965) [30]	3149 ± 20	• Thermal arrest (thermal analysis) when decreasing the temperature • Induction furnace	• UO_2 0.003 • W closed container (thick walls) or Re	• Composition analysis before and after by calcination • Analysis of W and Re inclusions

(*continued on next page*)

Table 3 (*continued*)

Authors year [Refs.]	Melting temperature (K)	Experimental technique	Sample preparation and container	Sample analysis
Bates (1966) [23]	3077 ± 25	• Visual observation of melting by long focal distance microscope • V shaped W ribbon • Ar-8% H_2 (1 bar)	• O/U ratio by calcination • Open system in W ribbon	
Bannister (1967) [22]	3133 ± 7	• Visual observation of melting by image projection • V shaped W ribbon • Neutral gas (1 bar)	• $UO_{2\pm0.21}$ by arc-melting of $UO_2 + U$ mixtures • Open system	• Analysis by calcination
Kjaerheim and Rolstad (1969) [38]	3138	• Thermal arrest • W furnace	• UO_2 sintered • Closed?	• DRX
Latta and Fryxell (1970) [9]	3138 ± 15	• Thermal arrest when decreasing the temperature • Induction furnace	• $UO_{1.998\pm0.003}$ • W (or Re) closed container	• Analysis before and after by calcinations • Analysis of W and Re inclusions
Bates (1970) [39]	3073 ± 20	• Visual observation of the melting • V shaped W ribbon • Ar (1 bar)	• UO_2 and irradiated samples • 87–95% theoretical density • Open system	• Analysis by calcination
Kapil (1976) [40]	3115	• Critical assessment		
Tachibana et al. (1985) [41]	3118 ± 25	• Thermal arrest • Induction furnace • Vacuum	• UO_2 (9g) • W closed container	
Komatsu et al. (1988) [42]	3115 ± 25	• Ditto	• Ditto	
Yamamoto et al. (1993) [43]	3118 ± 12	• Ditto	• Ditto	
Ronchi et al. (1993) [44]	3225 ± 15	• Laser heating and thermal arrest • C_p measurements	• Very small UO_2 balls (1 mm diameter)	• Not possible
Matzke et al. (1993) [45]	3140 ± 15	• Ditto	• Ditto	• Ditto
Halton et al. (1995) [46]	3152 ± 15	• Ditto	• Ditto	• Ditto
Manara et al. (2003/2004) [48,49]	3147 ± 20	• Laser heating of a surface • Thermal arrest (pyrometry on the surface)	• Sample in a high pressure cell (0.25 G Pa^{-1}) • Extrapolation to null pressure (= vacuum)	• Calcination at 1173 K by air in a thermobalance

*All temperature measurements were performed by pyrometry. In Refs. [9,30,32,37,39,42–44] a black body was used.

Table 4
Selected melting temperature for UO_2 from this literature analysis with mean values

Authors (date) [Refs.]	Melting $T \pm \delta T$ (K)
Hein et al. (1968) [49]	3138 ± 30
Kjaerheim and Rolstad (1969) [38]	3138 ± 20
Latta and Fryxell (1970) [9]	3138 ± 15
Tachibana et al. (1985) [41]	3118 ± 25
Matzke et al. (1993) [45]	3140 ± 15
Mean value	3134 ± 22[a]

N.B. For consistent data with retained values for the phase diagram, the data of Latta and Fryxell [9] are finally proposed for the melting temperature (see text).

[a] $\delta T = \pm 22$ K obtained using the law of propagation of errors.

according to the authors a melting temperature equal to 3147 K for UO_2 under null pressure (vacuum like conditions) and a variation according to the relation

$$dT_m/dp = 92.9 \pm 17.0 \text{ K GPa}^{-1}. \quad (4)$$

The melting temperature is higher by 9 K than the one retained in this study, meanwhile the slope agrees fairly well with the calculated one from our retained melting temperature and entropy, i.e. 92.3 K GPa^{-1}. However we have to quote that the slope is obtained for largely scattered data ($\sim\pm$20 K). For pressures lower than 0.05 Gpa the

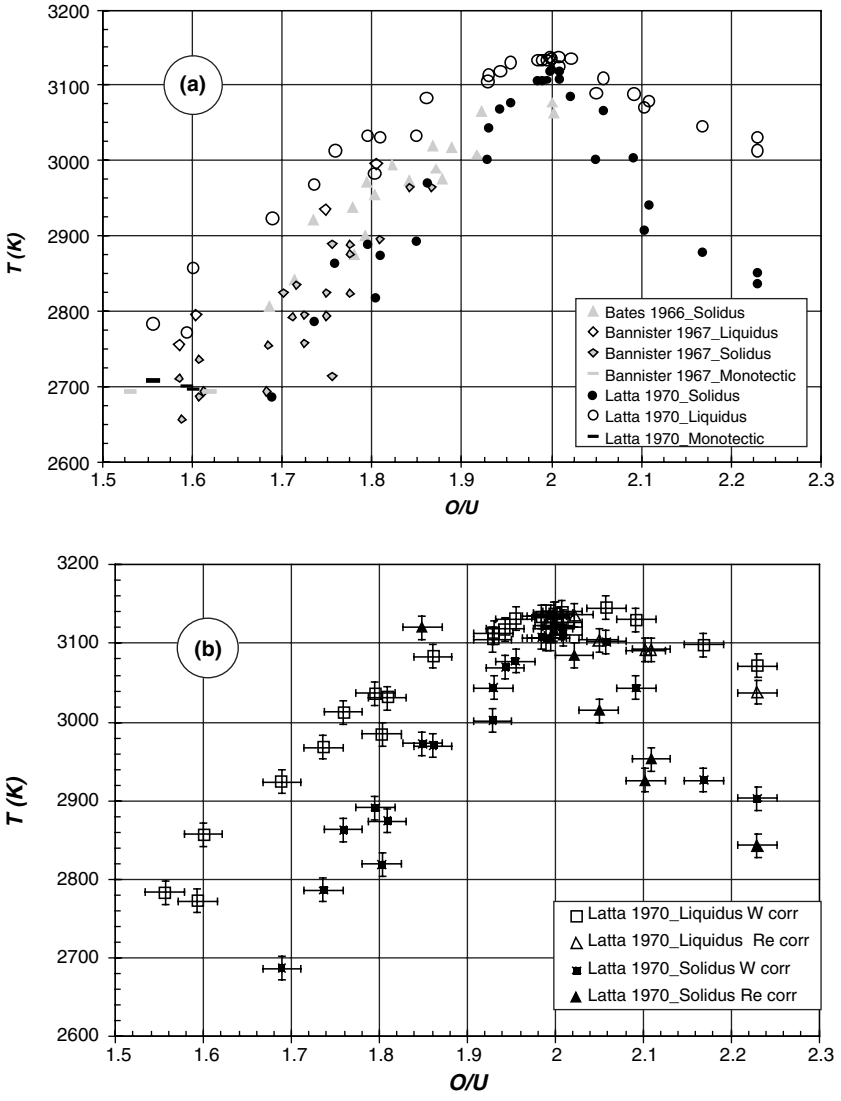

Fig. 6. (a) The whole set of liquidus and solidus data near the UO_2 composition and (b) retained and corrected solidus and liquidus data from Latta and Fryxell [9,30] with their estimated uncertainties.

Table 5
Liquidus temperatures of Latta and Fryxell [9,30] corrected using the Raoult's cryoscopic law from measured concentrations of dissolved W or Re

O/U	Cell	Original liquidus T (K)	Corrected		
			Molar % dissolved	ΔT	Liquidus T (K)
2.230	Re	3031	0.670	7	3038
2.230	W	3013	5.560	58	3071
2.169	W	3045	5.020	53	3098
2.109	Re	3078	1.370	14	3092
2.103	Re	3071	2.000	21	3092
2.092	W	3088	3.940	43	3131
2.050	Re	3090	1.340	14	3104
2.058	W	3109	3.320	36	3145
2.022	Re	3136	0.003	0	3136
2.009	W	3125	0.260	3	3128
1.998	Re	3138	0.005	0	3138
2.008	W	3138	0.250	3	3141
2.000	W	3135	0.240	3	3138
1.995	Re	3133	0.004	0	3133
1.990	W	3133	0.150	2	3135
1.985	W	3133	0.148	2	3135
1.955	W	3130	0.120	1	3131
1.943	W	3118	0.046	0	3118
1.930	W	3113	0.060	1	3114
1.929	W	3105	0.000	0	3105
1.861	W	3083	0.020	0	3083
1.795	W	3033	0..378	4	3037
1.849	W	3033	8.000[a]	87	3120
1.809	W	3031	0.014	0	3031
1.803	W	2983	0.140	1	2984
1.759	W	3013	0.007	0	3013
1.736	W	2968	0.012	0	2968
1.689	W	2923	0.064	1	2924
1.600	W	2857		0	2857
1.556	W	2783		0	2783
1.593	W	2771	0.198	2	2773

[a] This value seems abnormal and has been discarded from the retained final set.

decrease of melting temperature is attributed to composition evolution due to vaporisation losses. The authors further used higher pressures (>0.05 GPa) for measurements with UO_{2+x} samples in order to maintain negligible evaporation losses.

In order to compare the liquidus and solidus values proposed by Manara et al. (Table 6) with our selection, we first scaled their temperature values on the retained melting temperature in this work (decreasing by 9 K their original value), and second we applied a correction for null pressure according to present relation 4, assuming that the contribution for mixing entropy to the slope is small. Results are compared to our retained values of Latta and Fryxell in Fig. 7. The uncertainty for temperature measurements is the one proposed by the authors (±20 K) with an additional contribution equal to the difference observed for the melting temperature, i.e. 9 K: total uncertainty ±29 K. For composition the uncertainty proposed by the authors (±0.005) is retained, but the compositions are shifted according to the correction proposed by Labroche et al. [5].

In Fig. 7, we observe a clear disagreement, the Manara et al. values being systematically lower than those retained from Latta and Fryxell. According to our preceding analysis of congruent vaporisation, any composition evolution by matter loss should be toward UO_2 and consequently should give higher liquidus temperatures. As Manara et al. checked that no evolution of the measured temperatures occurred for pressures >0.05 Gpa, we can conclude that these determinations have been performed at constant compositions. Besides, from thermodynamic considerations – mainly Raoult's law –, the Latta and Fryxell determinations remain a lower bond in case of interactions occurring with the container and/or a small solubility at least in the liquid phase. We observe that the liquidus as proposed by Manara et al. and corrected by us, agrees fairly well with the solidus as retained from Latta and Fryxell. Therefore we can postulate that Manara et al. observed probably the disappearance of the liquid phase due to a change of the refraction index or total emissivity (liquid to solid), when assuming that the observed break corresponds to the disappearance of the liquid phase, i.e. the observation of the solidus. In that case, what happens at the second break? The real nature of the phenomena occurring for the two temperature breaks cannot probably be ruled out.

Another argument may be proposed that explains the low temperature data as proposed by Manara et al.: the starting temperature for the thermal analysis is very high, and combined to a large quenching speed, it is possible to favour the determination of a metastable phase diagram due to problems in the growth of the solid phase.

As a final argument, the authors propose a possibility of time limited composition segregation – the liquid is to be enriched with oxygen when freezing – that may not only influence the uncertainty in the retained composition values but also let unknown the real composition of the liquid droplet. They propose some complementary detailed microscopic analysis [48].

Table 6
Liquidus determinations from Manara et al. [48,49] and our proposed corrections as explained in the text

Sample composition (authors) O/U	Sample composition (this work) corrected for calcinations O/U corrected	Total applied pressure Gpa	Liquidus temperature (authors) T/K	Corrected with dP/dT (this work) T/K	Scaled liquidus with our melting temperature T/K
2	1.989	0.1	3147	3147	3138
2.01	1.999	0.1	3135	3126	3117
2.03	2.019	0.1	3130	3121	3112
2.03	2.019	0.15	3115	3101	3092
2.05	2.039	0.1	3098	3089	3080
2.07	2.059	0.05	3028	3023	3014
2.07	2.059	0.1	3070	3061	3052
2.07	2.059	0.2	3063	3045	3036
2.08	2.069	0.1	3075	3066	3057
2.09	2.079	0.1	3056	3047	3038
2.11	2.099	0.1	2995	2986	2977
2.12	2.109	0.1	3008	2999	2990
2.12	2.109	0.12	3020	3009	3000
2.14	2.129	0.1	2930	2921	2912
2.16	2.149	0.1	2920	2911	2902
2.17	2.159	0.05	2887	2882	2873
2.17	2.159	0.1	2891	2882	2873
2.17	2.159	0.2			
2.2	2.189	0.1	2865	2856	2847
2.21	2.199	0.1	2795	2786	2777

(i) Scaling to our retained melting temperature under null pressure and (ii) additional correction for null pressure according to relation (4).

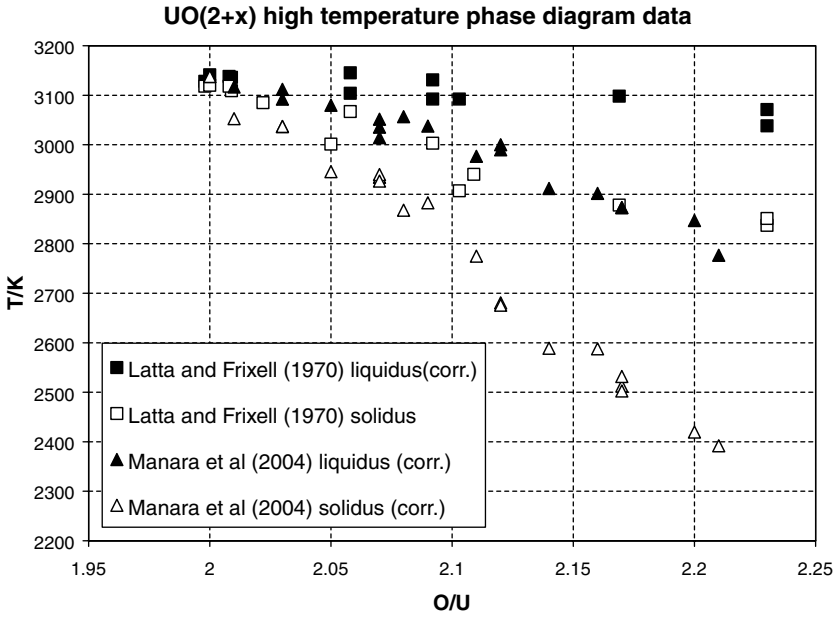

Fig. 7. Comparison between our selected values for the hyperstoichiometric UO_{2+x} liquidus and solidus (from Latta and Fryxell [9,30]) and the data from Manara et al. [53,54] performed by thermal analysis after Laser shots. We observe a coincidence of their liquidus data set with our selected solidus data set.

For all these reasons, we believe that the Manara et al. determinations of the liquidus and solidus cannot be retained to day, and complementary studies are needed.

4. The solubility limit of oxygen in liquid uranium

The determinations of the oxygen solubility in liquid uranium show very large discrepancies by factors of 10^2–10^3, as illustrated in Fig. 8. Indeed this solubility limit is an important property that determines the high temperature description of the liquid miscibility gap, as discussed in a preceding optimization and recent work [53] using two different data sets, which lead either to a large or a small miscibility gap. The different methods used to determine the solubility are presented in Table 7 and analyzed thereafter.

The results of Cleaves et al. [54] were obtained in the course of the Manhattan project during the Second World War with the device shown in Fig. 9. The BeO crucible was coated with a liner of UO_2 or sometimes with U_3O_8, which was obtained from a liquid/paste mixture deposited on the walls and sintered at 1973 K. Then the liquid U was equilibrated with the UO_2 (or U_3O_8) liner; this was sometimes assisted with an excess of O_2(g), directed through a tube on to the liquid surface; the experiment duration, ranged from 15 to 60 min. Then, the liquid U supposedly saturated with oxygen was extracted through a bottom hole and cooled quickly in a large conical shaped steel mould. The U solid ingot was then analyzed for oxygen content but also for other impurities such as Fe or C, from the mould. Different treatment durations (between 15 and 60 mn) gave the same oxygen content, showing that the thermodynamic equilibrium was already reached after 15 mn. Moreover, the O content was not varying whatever were the oxidizing conditions, UO_2 or U_3O_8 liner, or slight O_2 gas flow. However, high oxygen flow led to the formation of an oxide crust at the liquid surface. In this later case, the authors observed that the morphology of the UO_2 precipitates was clearly different from that obtained in the quenching process. It can be concluded that the UO_2 liner did not lead to any kind of spallation or particulate dissolution, probably due to its thinness and high density, and that the quenching process was efficient for sampling before chemical analysis of the whole ingot. The absence of solubility of BeO [62] in UO_2 also gives support to this conclusion.

Blum et al. [55] and Guinet et al. [58] melted large quantities of uranium in a thick sintered UO_2 crucible (Fig. 10). A low cooling speed is used, with or without a central frozen rod introduced at the top of the cell in order to observe, after the experiments, the crystallization morphology either from the crucible walls or from the rod or the surface of the liquid bath. Micrographic observations of the post-experiment ingot showed primary and secondary dendrites as well as UO_2 inclusions, probably from 'spallation' of the crucible walls when the metallic phase is stirred by the HF heating mode. The dendrites from the central rod or from the surface of the liquid could be related to the observations of Cleaves [54]; a UO_2 crust was formed at the surface under high oxygen content of the gas. The interface of the UO_2 crucible in contact with U liquid showed two layers. The first at the metallic side with pores and U(liq) penetration, in which

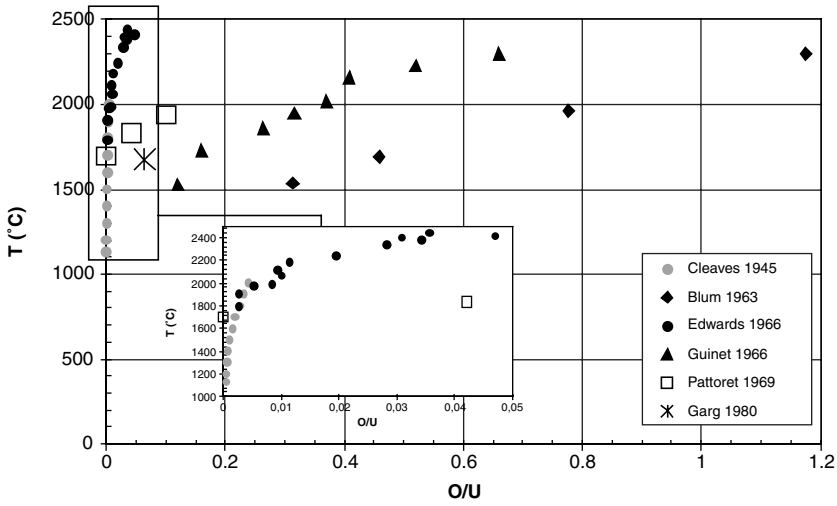

Fig. 8. Solubility limit of oxygen in liquid uranium according to experimental determinations.

Table 7
Experimental techniques used according to literature in the determination of oxygen solubility in U(1iq)

Authors (date) [Refs.]	Experimental technique and conditions	Container material	Temp. range (K) (number of data points)	Analytical techniques and characterization methods
Cleaves et al. (1945) [54]	• Heterogeneous equilibrium (saturation method) between U(1) and UO_2(s) as crucible • Induction furnace • Extraction through a bottom hole and quenching in a steel mould • He purified (1 bar), sometimes doped with O_2	• BeO with a thin liner of UO_2 or U_3O_8 • Prior heat treated at 1700°C	• 1404–2273 (10)	• Metallography • Chemical analysis of O content in U by vacuum fusion • Chemical analysis of Fe content • Check quenching in the mould
Blum et al. (1963) [55]	• Heterogeneous equilibrium U(1) in UO_2(s) crucible • Induction furnace • Slowly cooling or cooling by a central frozen rod • Ar purified (1 bar)	• UO_2 sintered	• 1809–2571 (4)	• Metallography • U ingot ground and analyzed for O content
Edwards and Martin (1965) [56] (1966) [57]	• Heterogeneous equilibrium of a U(l) small droplet with a UO_2single crystal cup • Quenching by switching off the W resistance furnace • He purified	• UO_2 single crystal cup	• 2063–2711 (13)	• Metallography • Chemical analysis of O content in the U droplet • UO_{2-x} melted an inert gas
Guinet et al. (1966) [58]	• Ditto Blum et al. [55]	• UO_2 sintered	• 1803–2573 (8)	• New interpretation of the crystallization morphology
Pattoret (1969) [20]	• Vapor pressure measurements of U(g) UO(g) and UO2(g) by Knudsen cell mass spectrometry • Use of the twin-cell method for activity measurements of U • Isothermal experiments with calibration and congruent composition determinations (polarography)	• Tungsten cells with different U or UO_{2-x} samples	• 1250–2250 (3) • 1970–2211 (3) liquidus	• Potentiometric analysis of the oxygen potential versus composition (UO_{2-x} solidus) • Use of Raoult law along the liquidus
Ackermann et al. (1965) [59]	• Vapor pressure measurements of U(g), UO(g) and UO2(g) by Knudsen cell mass spectrometry	• Tantalum cells (Ta or W crucibles)	• 1830–2500 (10)	• Potentiometric analysis of the oxygen potential versus composition (UO_{2-x} solidus)
Garg and Ackermann (1980) [31]	• Equilibration of U(l) and UO_2 (crucible) in a Ta Knudsen cell • Quenching (switching) off the furnace) and mass loss analysis by gravimetry	• UO_2 single crystal cup	• 1950 (1)	• Mass loss balance for the O content in U(l) • Calcinations for UO_{2-x} analysis

(*continued on next page*)

Table 7 (*continued*)

Authors (date) [Refs.]	Experimental technique and conditions	Container material	Temp. range (K) (number of data points)	Analytical techniques and characterization methods
Storms (1985) [60]	• Vapor pressure measurements of U(g), UO(g), UO_2(g) by Knudsen cell mass spectrometry	• Tungsten cells with UO_{2-x} and U–UO_2 samples	• 1667 – 2175 K	• Calcination under air at 1223 K
Guéneau et al. (1998) [61]	• Melting of U + UO_2 compacts by high power electron beam • Cooled Cu crucible • Vacuum quenching (switch off)	• No container (self crucible)	• 3100 ± 100K	• Metallography/ceramography • Microprobe analysis

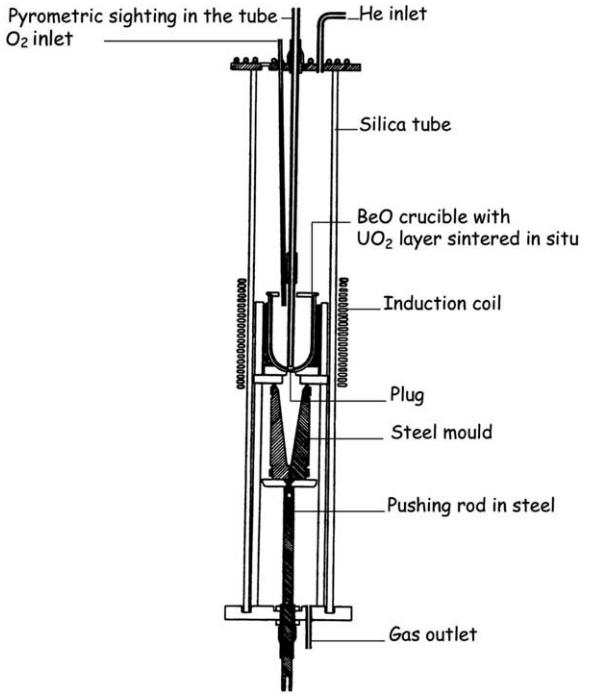

Fig. 9. Experimental set up as used by Cleaves et al. [56].

there was a detachment of further UO_2 inclusions such as a spallation process, and a second and dense layer close to the UO_2 phase, from which chemical analysis was performed to determine the solvus compositions, UO_{2-x}. All these observations, and some comparison with the experiment of Cleaves [54] under O_2 flow suggest that the present solubility limit of oxygen in liquid U proposed by Blum et al. may be significantly overestimated.

Edwards and Martin [57] equilibrated a small U liquid droplet with a UO_2 single crystal cup under He. The small quantity of matter, the small size of the tungsten resistor furnace, the fact that the U droplet spontaneously separated from the cup at quenching, all facilitated the oxygen analysis of the resulting U (droplet) phase and UO_{2-x} (cup) phase samples.

Garg and Ackermann [31] used UO_2 crucibles loaded with U in a tantalum effusion cell, and they observed that a long time was needed to form UO_{2-x} (solidus composition) from UO_2 Indeed, in case of very low solubility of oxygen in liquid uranium, the quantity of oxygen that can be dissolved in liquid U is not sufficient to allow the attainment of the UO_{2-x} solidus composition, and losses of matter by effusion (mainly UO(g)) were necessary to allow the process of oxygen loss of UO_{2-x} to

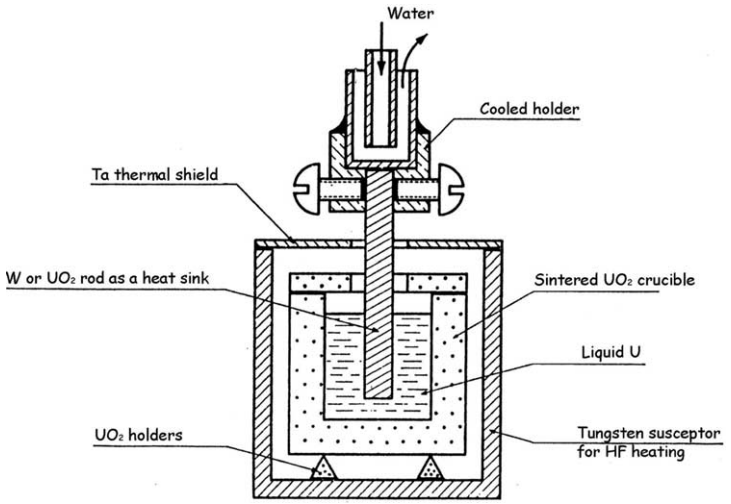

Fig. 10. Schematics of the liquid (U)–solid (UO_2) heterogeneous equilibrium device used by Blum et al. [57] and Guinet et al. [60] in a high frequency induction furnace.

be completed towards the solvus composition. Moreover, in the weight loss balance of the U and UO_2 phases as analyzed after the experiments in [31], the effusion loss had been computed on the basis of the partial pressure of UO(g), the values of which disagree by a factor 3 between different studies [14,15,63]. In addition, the Ta effusion cell reacted with the vapors, and UO(g) had been assumed to dissolve stoichiometrically in the Ta cell, while Edwards et al. [57] showed that only O is dissolved and diffuses through the cell walls. These two erroneous assumptions for correcting the mass balance of the U sample lead to large uncertainties in the solubility value, since these two above quantities are larger than the resulting solubility value (only about 30% of the total weight loss) and an overestimate of the solubility limit.

Pattoret [15] performed mass spectrometric measurements of the U activity in the diphasic $U(l) + UO_{2-x}(s)$ region by the twin Knudsen cell method [20,64]. Two tungsten cells were located in the same Ta isothermal envelope in a furnace that was moved in order to measure successively the ionic intensities I^+ of the same gaseous species ($\cong$ partial pressures). One cell was loaded with a diphasic $U(s) + UO_2(s)$ sample (previously equilibrated at high temperature) and the other with a pure U sample. First, the observation of the relative intensities of UO(g), U(g) and UO_2(g) as a function of time showed that U(1), probably covered initially with a thin UO_2 layer ($\cong$ 30–50 Å), lost oxygen by effusion. Indeed the diphasic partial pressures are such that the effusion flow composition is close to $O/U \sim 0.5$ (UO(g) being the main component) and the matter loss by vapor effusion is consequently richer in oxygen. After a while, the original pure U sample had lost enough oxygen to leave the diphasic $U + UO_2$ system and the purification of the liquid started: the partial pressure ratios

$$\frac{p(\mathrm{UO,g})}{p(\mathrm{U,g})} \quad \text{or} \quad \sqrt{\frac{p(\mathrm{UO_2,g})}{p(\mathrm{U,g})}} \tag{5}$$

proportional to the oxygen activity $\mathbf{a}_0$ decreased by a factor 2.3–7 (Table 8). At the same time, the activity of U is measured as the ratio,

$$a_{\mathrm{U}} = \frac{p_{\mathrm{U}}(\text{over } \mathrm{U} + \mathrm{UO_{2-x}})}{p_{\mathrm{U(pure\ U)}}} = \frac{I^+_{\mathrm{U}}(\mathrm{U} + \mathrm{UO_{2-x}})}{I^+_{\mathrm{U}}(\text{pure U})}. \tag{6}$$

In principle the purification process should finally produce a pure U(liq), and it is believed that the p(UO,g) and $p(UO_2$(g) final pressures observed by Pattoret et al. [20,64] after some time were either the residual contributions of parasitic re-vaporization after reaction of pure effused U(g) with the thermal shield materials [65] or a steady-state reaction with the residual oxygen in an isopiestic equilibrium with the vacuum pumping system [66]. These two processes could also operate together. The activities of U for the diphasic $U + UO_2$ referred to pure U as measured [20] are presented in Table 8 and the activity coefficient is calculated with

Table 8
Activity values of Pattoret [20] obtained by the twin Knudsen cell mass spectrometric method

T (K)	a_0[a] (Ref. U–UO_2)	a_U	Molar fraction of U at liquidus	Calculated activity coefficient of U		
			From [57]	From [55]	From [57]	From [55]
1970	0.43	1.0 ± 0.05	0.998	0.855	1.00 ± 0.05	1.17 ± 0.06
2107	0.21	0.96 ± 0.05	0.997	0.815	0.96 ± 0.05	1.18 ± 0.06
2211	0.14	0.91 ± 0.10	0.996	0.785	0.91 ± 0.11	1.16 ± 0.13

a_U is referred to U(1) in a W cell. a_0 is obtained from p_U/p_{UO_2} ratios from the diphasic U(1) + UO_2(s) sample in the second cell. The activity coefficient is then calculated from different solubility limits as proposed in Refs. [55] and [57].
[a] This activity is an indication of the purification of U(l) obtained by effusion loss of UO(g) and UO_2(g).

solubility values as proposed by Guinet et al. [58] and Edwards and Martin [57]. Using Raoult's law as a criterion, the consideration of large solubility values with the present activity values should lead to an activity coefficient $\gamma_U > 1$ which seems unrealistic owing to the strong interaction between oxygen and uranium. Thus, these measurements indicate the small solubility values to be the most thermodynamically compatible. However these U activity values cannot be retained in the further optimization procedure because their values, altogether with the relative large associated uncertainties, are too close to one, and that would finally lead to negligible weighting factors. Later,. the purification process by effusion was used again [67], in order to evaluate the solubility limit: a rough and rapid calculation of the total oxygen loss showed clearly a preferential agreement with Edwards and Martin data (See Table 8).

Recently, using high temperature equilibration techniques by high flow electron bombardment heating and quenching under vacuum (at these very high temperatures the radiation losses facilitate the quenching process) Guéneau et al. [61] observed the crystallization morphology and analyzed the chemical composition of the different phases obtained from the melting of an initial U + UO_2 mixed powder compacted sample. The 'as quenched' sample showed unambiguously an original equilibration morphology corresponding to a liquid miscibility gap and the resulting composition analysis of the two residues from liquids are in agreement with low solubility data of Edwards and Martin [57] and Cleaves [54]. The temperature is not very accurate (±100 K) because vaporization processes as well as short time sequences did not facilitate the pyrometric measurements. Concurrently, some vaporization simulations based on

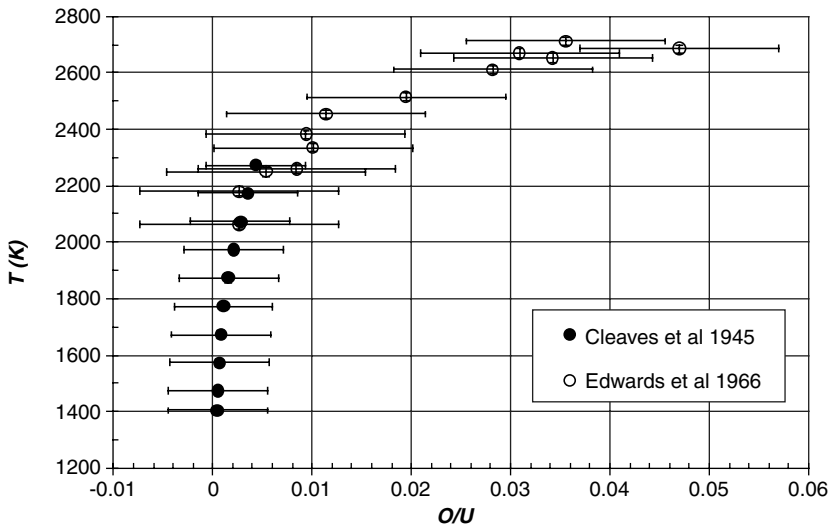

Fig. 11. Solubility of oxygen in liquid uranium data as retained in this work with their associated uncertainties.

sample weight losses and collection on targets disposed on the surrounding cold dome yielded a temperature evaluation in the same range than pyrometric measurements. It should be noted that, even if the temperature uncertainty seems large, its effect on the quasi-vertical miscibility gap lines in this range is not be very significant, and the composition analysis uncertainty remains small (the authors uncertainties are retained).

In conclusion, heterogeneous equilibria U(liq) – UO_{2-x} are retained for experiments performed with small samples and dense crucible materials, with efficient quenching and clear phase separation before chemical analysis, i.e. the experiments of Cleaves [54] and Edwards and Martin [57]. For compatibility reasons, the very high temperature results of Guéneau et al. [61] are also retained. Activity values obtained by Pattoret [20,64] combined with Raoult's law clearly delimit those results from those that cannot be correct, on the basis of the present analysis.

The uncertainties retained in Edwards and Martin [57] solubility determinations are those proposed by the authors and obtained from chemical analysis by arc melting, $\delta x = \pm 0.01$. We quote that this value is larger than proposed by Labroche et al. [3,5] in Table 1. In the Cleaves et al. [54] studies, two sources of uncertainties are proposed, firstly, the difference between the top and the bottom of the quenched ingots, $\delta x = \pm 0.005$ and secondly the blank that may become important for very low solubility data, $\delta x = \pm 0.005$. Applying the law of propagation of errors, the final attributed δx is ± 0.007. Temperature uncertainties retained for the two authors who used calibrated pyrometers is $\delta T = \pm 15$ K. The retained data with their associated uncertainties are in agreement as shown in Fig. 11.

5. UO_{2-x} solidus below the eutectic temperature

The different methods of measurements and their experimental conditions are presented in Table 7. These data (Fig. 12(a)) show general agreement except for Bates values [23] that appear largely scattered, and the analysis of the consistency of these data can only be performed once their uncertainties evaluated: the largest discrepancies noted are for temperatures >2400 K.

In the Martin and Edwards experiments [57], the UO_2 single crystal cup during the quenching process precipitates some U crystals that can oxidize, at least from their surface, when returned in air, before cleaning the U excess by HCl attack. Then the calcination process allows the O/U composition to be determined. Air exposure as well as HCl attack can thus lead to underestimate the real U content of the UO_{2-x} cup, and this underestimate increases with U content or temperature due to the solidus shape. So, it is believed that the five data at high temperature, which are less U rich, should be discarded. The total uncertainty for $T > 2400$ K is calculated according to those mentioned in Tables 1 and 2 in which a correction (± 0.0133) of half that of Ackermann and Chang is arbitrarily chosen for a usual calcination temperature at that time in the range 1173–1273 K (this temperature is not published by Martin and Edwards)

$$\delta x(T > 2400\ \mathrm{K}) = \pm\sqrt{\left((0.003)^2 + (0.002)^2 + (0.002)^2 + (0.0133)^2\right)} = \pm 0.014. \quad (7)$$

For temperatures lower than 2400 K

$$\delta x(T > 2400\ \mathrm{K}) = \pm\sqrt{\left((0.003)^2 + (0.0133)^2\right)} = \pm 0.014. \quad (8)$$

From this uncertainty estimate the preceding discarded five data become non-compatible with other data.

Guinet et al. [58] analyzed the UO_{2-x} compact layer at the inner wall of the UO_2 crucible material in contact with U after the experiment, this layer being carefully separated from the preceding one on the liquid side intermixed with U(s). The uncertainty combines air exposure and vacuum fusion analysis for the O/U ratio

$$\delta x = \pm\sqrt{\left((0.002)^2 + (0.006)^2\right)} = \pm 0.006. \quad (9)$$

Ackermann et al. [63], Drowart et al. [14], Pattoret [20] and Storms [60] determined the solvus composition by potentiometric analysis: vapor pressure measurements by mass spectrometry obtained as a function of temperature for constant compositions were displayed versus composition and their intercept with the diphasic U–UO vapor pressure retained. Thus, the uncertainty for the T intercept determination is fixed at twice the uncertainties of temperature measurements. For the composition analysis, Storms calcined at 1223 K, while Ackermann et al. used calcination at an unpublished

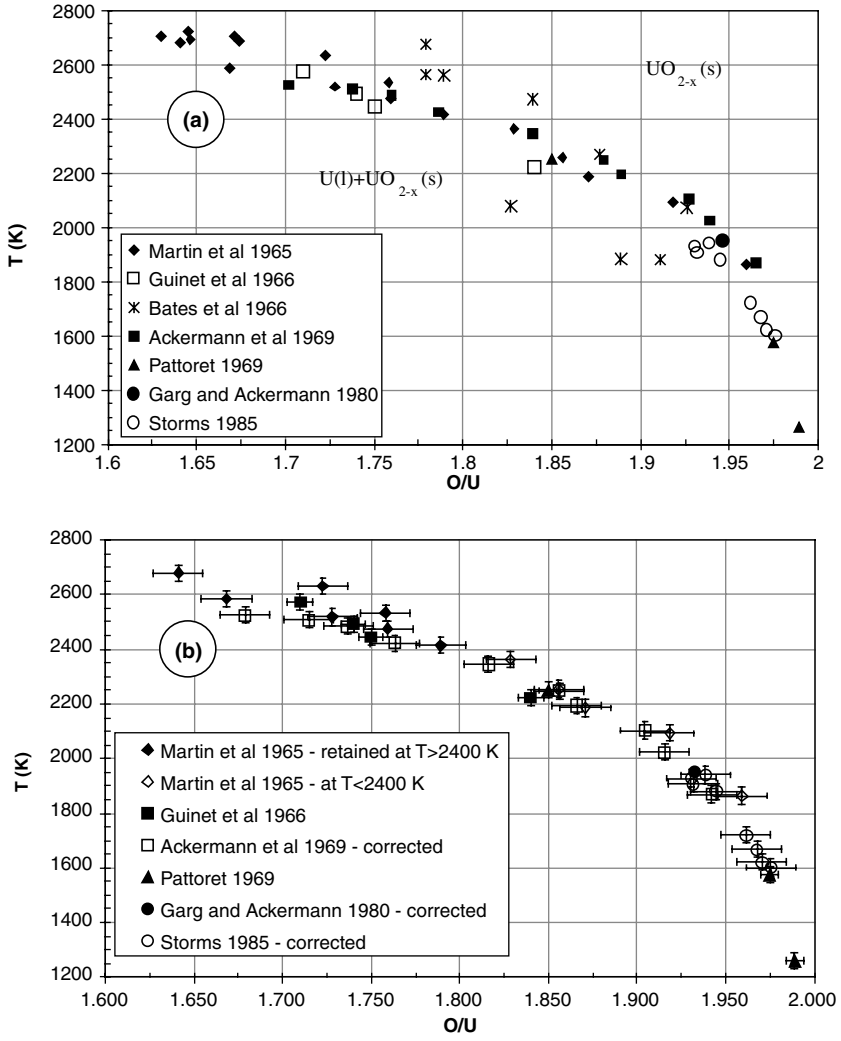

Fig. 12. (a) All solvus data original (before selection and correction), (b) UO_{2-x} retained solvus data with the uncertainties attributed to each author.

temperature but usually around 1173–1273 K at that time: consequently these two sets of values are corrected with half the Ackermann and Chang correction (−0.0133). Thus half the Ackermann and Chang correction plus the air exposure uncertainty is taken into account in the incertainty here:

$$\delta x = \pm\sqrt{\left((0.003)^2 + (0.002)^2 + (0.0133)^2\right)} = \pm 0.014 \quad (10)$$

and for Drowart et al. [14] and Pattoret [20], the polarographic analysis and the air exposure,

$$\delta x = \pm\sqrt{\left((0.005)^2 + (0/002)^2\right)} = \pm 0.0053. \quad (11)$$

In the Garg and Ackermann [31] experiment, the calcination of the UO_2 cup after quenching does not depend on the interactions of the U–O vapors with the Ta cell as well as on the oxygen balance in the experiment. Their data, consistent with other studies, attest that the entire cup reached the solidus composition. The uncertainty takes into account air exposure, calcination analysis (Ackermann and Chang correction) and authors uncertainties:

$$\delta x = \pm\sqrt{\left((0.003)^2 + (0.002)^2 + (0.0133)^2\right)} = \pm 0.014. \quad (12)$$

In order to be consistent with the Ackermann and Chang half uncertainty when attributed to calcina-

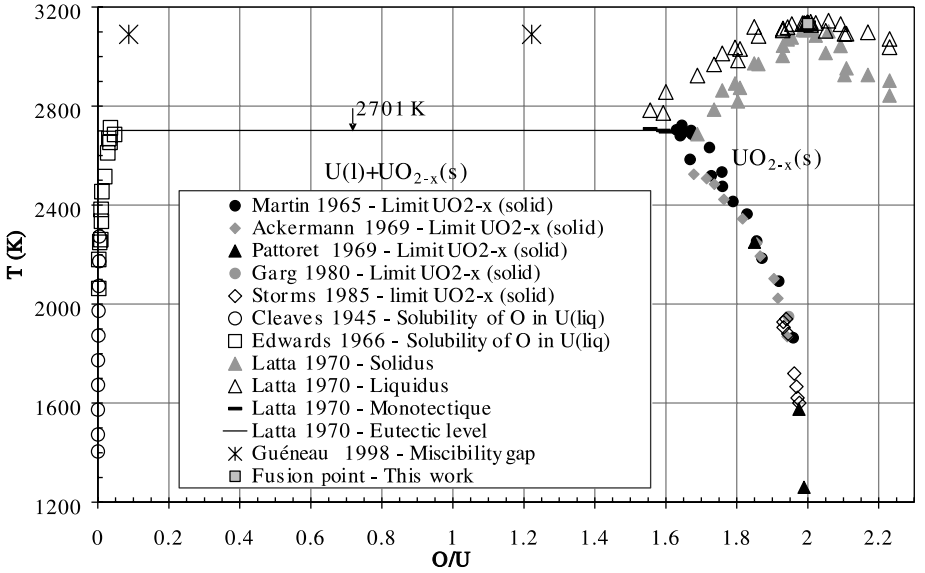

Fig. 13. Phase diagram data retained in this work for the U–UO_2 range.

tion, it is important to quote again that the second half part of the uncertainty is used to correct the original data directly.

The Bates [23] values are not retained due to large scatter and difficulties to attribute a realistic uncertainty.

The retained values with their associated uncertainties are presented in Fig. 12(b). We observe that systematically the correction used in this paper for composition analysis by calcinations the 'Ackermann and Chang correction' tends to render more consistent all the retained values.

6. Conclusion on phase diagram data

Large discrepancies on phase diagram data in the U–UO_2 range have been discussed and careful analysis of experimental conditions as well as suitable comparison of all the results allowed the selection of a set of reliable data leading to the phase diagram as presented in Fig. 13 and optimized in Ref. [28].

A major cause of discrepancies has been attributed to the calcination method for composition determinations and the proposed 'Ackermann and Chang' half correction improved seriously the consistency of the retained data sets from different authors.

A special effort has been made in the evaluation of the associated uncertainties for each data set in order to aid in the selection of consistent primary data and in the use of these uncertainties as weights in the optimization procedure [28] performed on thermodynamic and phase diagram data. All assessed experimental values for phase diagram in the U–UO_{2+x} composition range are reported in Appendix A together with their assigned uncertainties.

Acknowledgements

The authors acknowledge Dr Paul Potter for help in the preparation of the final text.

Appendix A

Assessed experimental values for the phase diagram in the U–UO_{2+x} composition range and their assigned uncertainties

Authors (date) [Refs.]	Type of data	O/U	δ(O/U)	T (K)	δT
This work	Melting point	2.000	0.002	3134	22
Latta and Fryxell (1970) [9]	Solidus original	2.230	0.022	2837	15

(*continued on next page*)

Appendix A (*continued*)

Authors (date) [Refs.]	Type of data	O/U	δ(O/U)	T (K)	δT
	Solidus original	2.230	0.022	2851	15
	Solidus original	2.169	0.022	2878	15
	Solidus original	2.109	0.022	2940	15
	Solidus original	2.103	0.022	2907	15
	Solidus original	2.092	0.022	3003	15
	Solidus original	2.050	0.022	3001	15
	Solidus original	2.058	0.022	3067	15
	Solidus original	2.022	0.022	3085	15
	Solidus original	2.009	0.022	3109	15
	Solidus original	1.998	0.022	3118	15
	Solidus original	2.008	0.022	3118	15
	Solidus original	2.000	0.022	3120	15
	Solidus original	1.995	0.022	3107	15
	Solidus original	1.990	0.022	3105	15
	Solidus original	1.985	0.022	3106	15
	Solidus original	1.955	0.022	3076	15
	Solidus original	1.943	0.022	3069	15
	Solidus original	1.930	0.022	3043	15
	Solidus original	1.929	0.022	3002	15
	Solidus original	1.861	0.022	2970	15
	Solidus original	1.795	0.022	2888	15
	Solidus original	1.849	0.022	2893	15
	Solidus original	1.809	0.022	2874	15
	Solidus original	1.803	0.022	2818	15
	Solidus original	1.759	0.022	2863	15
	Solidus original	1.736	0.022	2786	15
	Solidus original	1.689	0.022	2686	15
	Solidus original	2.230	0.022	2837	15
	Solidus original	2.230	0.022	2851	15
	Solidus original	2.169	0.022	2878	15
	Solidus original	2.109	0.022	2940	15
Latta and Fryxell (1970) [9]	Liquidus W corrected [(a)]	2.230	0.022	3071	15
	Liquidus W corrected [(a)]	2.169	0.022	3098	15
	Liquidus W corrected [(a)]	2.092	0.022	3131	15
	Liquidus W corrected [(a)]	2.058	0.022	3145	15
	Liquidus W corrected [(a)]	2.009	0.022	3128	15
Latta and Fryxell (1970) [9]	Liquidus W corrected [(a)]	2.008	0.022	3141	15
	Liquidus W corrected [(a)]	2.000	0.022	3138	15
	Liquidus W corrected [(a)]	1.990	0.022	3135	15
	Liquidus W corrected [(a)]	1.985	0.022	3135	15
	Liquidus W corrected [(a)]	1.955	0.022	3131	15
	Liquidus W corrected [(a)]	1.943	0.022	3118	15
	Liquidus W corrected [(a)]	1.930	0.022	3114	15
	Liquidus W corrected [(a)]	1.929	0.022	3105	15
	Liquidus W corrected [(a)]	1.861	0.022	3083	15
	Liquidus W corrected [(a)]	1.795	0.022	3037	15
	Liquidus W corrected [(a)]	1.809	0.022	3031	15

Appendix A (*continued*)

Authors (date) [Refs.]	Type of data	O/U	δ(O/U)	T (K)	δT
	Liquidus W corrected [a]	1.803	0.022	2984	15
	Liquidus W corrected [a]	1.759	0.022	3013	15
	Liquidus W corrected [a]	1.736	0.022	2968	15
	Liquidus W corrected [a]	1.689	0.022	2924	15
	Liquidus W corrected [a]	1.600	0.022	2857	15
	Liquidus W corrected [a]	1.556	0.022	2783	15
	Liquidus W corrected [a]	1.593	0.022	2773	15
	Liquidus Re corrected [a]	2.230	0.022	3038	15
	Liquidus Re corrected [a]	2.109	0.022	3092	15
	Liquidus Re corrected [a]	2.103	0.022	3092	15
	Liquidus Re corrected [a]	2.050	0.022	3104	15
	Liquidus Re corrected [a]	2.022	0.022	3136	15
	Liquidus Re corrected [a]	1.998	0.022	3138	15
	Liquidus Re corrected [a]	1.995	0.022	3133	15
Latta and Fryxell (1970) [9]	Monotectic	1.600	0.022	2696	15
	Monotectic	1.556	0.022	2708	15
	Monotectic	1.593	0.022	2701	15
Guéneau et al. (1998) [61]	Miscibility gap	0.087	0.020	3090	100
	Miscibility gap	1.222	0.020	3090	100
Martin and Edwards (1965) [56]	Limit UO_{2-x}(solid)	1.959	0.014	1864	30
	Limit UO_{2-x}(solid)	1.918	0.014	2092	30
	Limit UO_{2-x}(solid)	1.871	0.014	2186	30
	Limit UO_{2-x}(solid)	1.856	0.014	2255	30
	Limit UO_{2-x}(solid)	1.829	0.014	2364	30
	Limit UO_{2-x}(solid)	1.789	0.014	2414	30
	Limit UO_{2-x}(solid)	1.759	0.014	2475	30
	Limit UO_{2-x}(solid)	1.758	0.014	2534	30
	Limit UO_{2-x}(solid)	1.728	0.014	2518	30
	Limit UO_{2-x}(solid)	1.723	0.014	2632	30
	Limit UO_{2-x}(solid)	1.668	0.014	2584	30
	Limit UO_{2-x}(solid)	1.641	0.014	2680	30
	Limit UO_{2-x}(solid)	1.647	0.014	2691	30
	Limit UO_{2-x}(solid)	1.630	0.014	2704	30
	Limit UO_{2-x}(solid)	1.645	0.014	2723	30
	Limit UO_{2-x}(solid)	1.671	0.014	2701	30
	Limit UO_{2-x}(solid)	1.674	0.014	2685	30
Guinet et al. (1966) [58]	Limit UO_{2-x}(solid)	1.840	0.007	2223	30
	Limit UO_{2-x}(solid)	1.750	0.007	2443	30
	Limit UO_{2-x}(solid)	1.740	0.007	2493	30
	Limit UO_{2-x}(solid)	1.710	0.007	2573	30
	Monotectic (1)	1.180	0.007	2470	30
Ackermann et al. (1969) [63]	Limit UO_{2-x}(solid) corrected [b]	1.702	0.014	2525	30
	Limit UO_{2-x}(solid) corrected [b]	1.738	0.014	2508	30
	Limit UO_{2-x}(solid) corrected [b]	1.760	0.014	2485	30
	Limit UO_{2-x}(solid) corrected [b]	1.786	0.014	2423	30

(*continued on next page*)

Appendix A (*continued*)

Authors (date) [Refs.]	Type of data	O/U	δ(O/U)	T (K)	δT
	Limit UO_{2-x}(solid) corrected [b]	1.839	0.014	2345	30
	Limit UO_{2-x}(solid) corrected [b]	1.879	0.014	2248	30
	Limit UO_{2-x}(solid) corrected [b]	1.889	0.014	2194	30
	Limit UO_{2-x}(solid) corrected [b]	1.927	0.014	2103	30
	Limit UO_{2-x}(solid) corrected [b]	1.939	0.014	2023	30
	Limit UO_{2-x}(solid) corrected [b]	1.965	0.014	1869	30
Garg and Ackermann (1980) [31]	Limit UO_{2-x}(solid) corrected [b]	1.932	0.014	1950	30
Pattoret (1969) [20]	Limit UO_{2-x}(solid)	1.850	0.020	2250	30
	Limit UO_{2-x}(solid)	1.975	0.005	1575	30
	Limit UO_{2-x}(solid)	1.989	0.005	1260	30
Storms (1985) [60]	Limit UO_{2-x}(solid) corrected [b]	1.931	0.014	1928	30
	Limit UO_{2-x}(solid) corrected [b]	1.932	0.014	1906	30
	Limit UO_{2-x}(solid) corrected [b]	1.939	0.014	1940	30
	Limit UO_{2-x}(solid) corrected [b]	1.945	0.014	1880	30
	Limit UO_{2-x}(solid) corrected [b]	1.962	0.014	1720	30
	Limit UO_{2-x}(solid) corrected [b]	1.968	0.014	1667	30
	Limit UO_{2-x}(solid) corrected [b]	1.971	0.014	1621	30
	Limit UO_{2-x}(solid) corrected [b]	1.976	0.014	1601	30
Cleaves et al. (1945) [54]	Solubility of O in U(liq)	0.00046	0.010	1404	15
	Solubility of O in U(liq)	0.00052	0.010	1473	15
	Solubility of O in U(liq)	0.00063	0.010	1573	15
	Solubility of O in U(liq)	0.00079	0.010	1673	15
	Solubility of O in U(liq)	0.00107	0.010	1773	15
	Solubility of O in U(liq)	0.00156	0.010	1873	15
	Solubility of O in U(liq)	0.00208	0.010	1973	15
	Solubility of O in U(liq)	0.00281	0.010	2073	15
	Solubility of O in U(liq)	0.00351	0.010	2173	15
	Solubility of O in U(liq)	0.00434	0.010	2273	15
Edwards and Martin (1966) [57]	Solubility of O in U(liq)	0.00268	0.010	2063	15
	Solubility of O in U(liq)	0.00268	0.010	2180	15
	Solubility of O in U(liq)	0.00537	0.010	2249	15
	Solubility of O in U(liq)	0.00846	0.010	2260	15
	Solubility of O in U(liq)	0.01007	0.010	2334	15
	Solubility of O in U(liq)	0.00940	0.010	2382	15
	Solubility of O in U(liq)	0.01141	0.010	2454	15
	Solubility of O in U(liq)	0.01946	0.010	2515	15
	Solubility of O in U(liq)	0.02819	0.010	2611	15
	Solubility of O in U(liq)	0.03423	0.010	2654	15
	Solubility of O in U(liq)	0.03087	0.010	2669	15
	Solubility of O in U(liq)	0.04698	0.010	2685	15
	Solubility of O in U(liq)	0.03557	0.010	2712	15

[a] Correction according to Raoult's law.
[b] Correction according to insufficient calcinations into U_3O_8 as evidenced by Ackermann and Chang [6] and discussed by Labroche et al. [3]: ($O/U^{corrected} = O/U^{original} - 0.0133$).

References

[1] B. Jansson, Report TRITA-MAC-0234, Materials Center, Royal Institute of Technology, S10044 Stockholm 70, Sweden, 1984, 25p.
[2] M. Baïchi, Ph.D, Contribution à l'étude du corium d'un réacteur nucléaire accidenté: aspects puissance résiduelle et thermodynamique des systèmes U–UO_2 et UO_2-ZrO_2, Institut National Polytechnique de Grenoble, Grenoble, France (24th Sept. 2001).
[3] D. Labroche, Ph.D, Contribution à l'étude thermodynamique du système ternaire U–Fe–O, Institut National Polytechnique de Grenoble, Grenoble, France, 29th September 2000.
[4] E.A. Schaefer, J.O. Hibbits, Anal. Chem. 41 (1969) 254.
[5] D. Labroche, J. Nucl. Mater. 312 (2003) 21.
[6] R.J. Ackermann, A.T. Chang, J. Chem. Thermodyn. 5 (1973) 873.
[7] P. Gerdanian, M. Dodé, J. Chim. Phys. (1965) 171.
[8] P. Srirama Murti, R.B. Yadav, H.P. Nawada, Thermochim. Acta 140 (1989) 299.
[9] R.E. Latta, R.E. Fryxell, J. Nucl. Mater. 35 (1970) 195.
[10] F. Rossini, Assignement of Uncertainties to Thermochemical Data, in Experimental Thermochemistry Measurement of Heats of Reaction, Interscience Publishers, Ltd. and Carnegie Institute of Technology, New York and Pittsburgh, Pennsylvania, 1956, p. 297.
[11] R.J. Ackermann, P.W. Gilles, R.J. Thorn, J. Chem. Phys. 25 (1956) 1089.
[12] R.N. Duncan, H.M. Ferrari, Trans. Am. Nucl. Soc. 6 (1963) 152.
[13] J.A. Christensen, Report HW-69234 (1962) 24.
[14] J. Drowart, A. Pattoret, S. Smoes, Mass Spectrometric Studies of the Vaporization of Refractory Compounds, in: Proceedings of the Ceramic Society, Proceedings of the Ceramic Society, New York, 1967, p. 67.
[15] A. Pattoret, J. Drowart, S. Smoes, Bull. Soc. Fr. Ceram. 77 (1967) 75.
[16] I. Prigogine, R. Defay, Azéotropie, in: Thermodynamique chimique, Dunod, Paris, 1950, p. 477.
[17] D.H. Everett, Azeotropy, in: Chemical Thermodynamics, Longmans, London, 1965, p. 450.
[18] I. Prigogine, R. Defay, Les états indifférents, in: Thermodynamique chimique, Dunod, Paris, 1950, p. 498.
[19] D.H. Everett, Indifferent States, in: Chemical Thermodynamics, Longmans, London, 1695, p. 468.
[20] A. Pattoret, Ph. D, Etudes Thermodynamiques par Spectrométrie de Masse sur les Systèmes Uranium–Oxygène et Uranium–Carbone, Université Libre de Bruxelles, Belgique, 20th May 1969.
[21] R.K. Edwards, M.S. Chandrasekharaiah, P.M. Danielson, High Temp. Sci. 1 (1969) 98.
[22] M.J. Bannister, J. Nucl. Mater. 24 (1967) 340.
[23] J.L. Bates, J. Am. Ceram. Soc. 49 (1966) 395.
[24] C. Younés, Ph. D, Contribution à l'étude thermodynamique par spectrométrie de masse à haute température des oxydes MO2-x [M= U, (U,La), (La,Ce), (La,Ce,Y), (U,Ce)], Université de Paris-Sud, Orsay, France, 26th June 1986.
[25] R.J. Ackermann, E.G. Rauh, M.H. Rand, A re-determination and re-assessment of the thermodynamics of sublimation of uranium dioxideThermodynamics of Nuclear Materials 1979, 1, IAEA, Vienna, 1980, p. 11.
[26] J.S. Anderson, J.O. Sawyer, H.W. Worner, G.M. Willis, M.J. Bannister, Nature 185 (1960) 915.
[27] E. Rothwell, J. Nucl. Mater. 6 (1962) 229.
[28] C. Guéneau, M. Baïchi, D. Labroche, C. Chatillon, B. Sundman, J. Nucl. Mater. 304 (2002) 161.
[29] J.Y. Shen, C. Chatillon, J. Cryst. Growth 106 (1990) 543.
[30] R.E. Latta, R.E. Fryxell, Trans. Am. Nucl. Soc. 8 (1965) 375.
[31] S.P. Garg, R.J. Ackermann, J. Nucl. Mater. 88 (1980) 309.
[32] W.A. Lambertson, M.H. Mueller, J. Am. Ceram. Soc. 36 (1953) 329.
[33] L.G. Wisnyi, S.W. Pijanowski, Report KAPL-1702 (1957) 20.
[34] T.C. Ehlert, J.L. Margrave, J. Am. Ceram. Soc. 41 (1958) 330.
[35] T.D. Chikalla, J. Am. Ceram. Soc. 46 (1963) 323.
[36] H. Hausner, J. Nucl. Mater. 15 (1965) 179.
[37] M.F. Lyons, B. Weidenbaum, H. Hausner, T.J. Pashos, Trans. Am. Nucl. Soc. 8 (1965) 376.
[38] G. Kjaerheim, E. Rolstad, Halden Report HPR-107 (1969) 36.
[39] J.L. Bates, J. Nucl. Mater. 36 (1970) 234.
[40] S.K. Kapil, J. Nucl. Mater. 60 (1976) 158.
[41] T. Tachibana, T. Ohmori, S. Yamanouchi, T. Itaki, J. Nucl. Sci. Technol. 22 (1985) 155.
[42] J. Komatsu, T. Tachibana, K. Konashi, J. Nucl. Mater. 154 (1988) 38.
[43] K. Yamamoto, K. Hirosawa, K. Morozumi, S. Nomura, J. Nucl. Mater. 204 (1993) 85.
[44] C. Ronchi, J.P. Hiernaut, R. Selfslag, G.J. Hyland, Nucl. Sci. Eng. 113 (1993) 1.
[45] Hj. Matzke, P.G. Lucuta, R.A. Verrall, J.P. Hiernaut, Thermophysical properties of UO_2 and SIMFUEL – simulated high-burnup fuel, in: Proceeding 22nd Int. Thermal Conductivity Conference, Tempe, Arizona, 7–10 November 1993.
[46] D. Halton, J.P. Hiernaut, M. Sheidlin, C. Ronchi, Advances in laser applications for high temperature thermophysical measurements in ceramics, in: Fourth Euro Ceramics, Karlsruhe, EEC Joint Research Society, 1995.
[47] M.H. Rand, R.J. Ackermann, F. Gronwold, F.L. Oetting, A. Pattoret, Rev. Int. Hautes Temp. Réfrac. Fr. 15 (1978) 335.
[48] D. Manara, C. Ronchi, M. Sheindlin, High Temp. High Press. 35&36 (2003/2004) 25.
[49] D. Manara, C. Ronchi, M. Sheindlin, M. Lewis, M. Brykin, J. Nucl. Mater. 342 (2005) 148.
[50] R.A. Hein, P.N. Flagella, Report GEMP-578 (1968) 11.
[51] L. Leibowitz, M.G. Chasanov, L.W. Mishler, D.F. Fischer, J. Nucl. Mater. 39 (1971) 115.
[52] L. Leibowitz, L.W. Mishler, M.G. Chasanov, J. Nucl. Mater. 29 (1969) 356.
[53] P.Y. Chevalier, E. Fischer, J. Nucl. Mater. 257 (1998) 213.
[54] H.E. Cleaves, M.M. Cron, J.T. Sterling, Report CT-2618 (1945) 16.
[55] P. Blum, P. Guinet, H. Vaugoyau, C.R. Acad. Sci. Paris 257 (1963) 3401.
[56] A.E. Martin, R.K. Edwards, J. Phys. Chem. 69 (1965) 1788.

[57] R.K. Edwards, A.E. Martin, Phase Relations in the Uranium–Uranium Dioxide System at High Temperatures, in Thermodynamics, International Atomic Energy Agency, (IAEA), Vienna, 1966, 423.
[58] P. Guinet, H. Vaugoyau, P. Blum, C.R. Acad. Sci. Paris 263 (1966) 17.
[59] R.J. Ackermann, E.G. Rauh, M.S. Chandrasekharaiah, Report ANL-7048 (1965) 33.
[60] E.K. Storms, J. Nucl. Mater. 132 (1985) 231.
[61] C. Guéneau, V. Dauvois, P. Pérodeaud, C. Gonella, O. Dugne, J. Nucl. Mater. 254 (1998) 158.
[62] E.M. Levin, C.R. Robbins, H.F. McMurdie, System BeO–UO_2, in Phase Diagram for Ceramists, The American Ceramic Society, Ohio, 1969, p. 101.
[63] R.J. Ackermann, E.G. Rauh, M.S. Chandrasekharaiah, J. Phys. Chem. 73 (1969) 762.
[64] A. Pattoret, J. Drowart, S. Smoes, Trans. Faraday Soc. 65 (1969) 98.
[65] C. Chatillon, M. Allibert, A. Pattoret, High Temp. Sci. 8 (1976) 233.
[66] R.J. Ackermann, E.G. Rauh, R.J. Thorn, J. Chem. Phys. 37 (1962) 2693.
[67] P. Gardie, Ph.D, Contribution à l'étude thermodynamique des alliages U–Fe et U–Ga par spectrométrie de masse à haute température, et de la mouillabilité de l'oxyde d'yttrium par l'uranium, Institut National Polytechnique de Grenoble, Grenoble, France, 23th October 1992.